SFR inferred from the far-infrared luminosity of 4C41.17 and the shape of the ultraviolet–optical SED are still consistent with an old galaxy (with formation redshift $z_f > 10$) undergoing a 10^6-yr starburst involving as little as 1% of the mass of the underlying galaxy.

Similar problems afflict attempts to determine the evolutionary state of 4C41.17 from its peculiar optical morphology. The rest-frame wavelength of the Hubble Space Telescope image reproduced in Fig. 2 is 1,400 Å, and even at $z < 1$ it is now well established that powerful radio galaxies frequently possess a component of ultraviolet light aligned with the radio structure[4] Our conclusion that the centre of the galaxy is concealed by a dust lane further weakens claims that its multi-modal optical structure is indicative of an elliptical galaxy in the process of formation. It also remains difficult to rule out the presence of a significant population of evolved stars, as even near-infrared observations of 4C41.17 (ref. 14) sample continuum light at a rest-frame wavelength of only 4,600 Å.

In principle, therefore, the most straightforward way to identify whether a galaxy at $z > 3$ is genuinely young is to determine what fraction of its final stellar mass has yet to be converted into stars at the epoch of observation. 4C41.17 certainly contains much more dust than has been found in low-redshift radio galaxies. Although the uncertainties involved in converting this dust mass into a gas mass are large (D.H.H., J.S.D. and S.R., manuscript in preparation), assuming a canonical gas to dust ratio of 500, which is supported by recent CO observations of 10214+4724 (ref. 28), leads to an estimate of the gas mass in 4C41.17 of $M_{gas} \approx 10^{11} M_{\odot}$. This value is at least consistent with the idea that a significant fraction (~10%) of the galaxy's eventual stellar mass has yet to be converted into stars at $z = 3.8$.

Thus, although our detection of dust in 4C41.17 indicates the occurrence of recent large-scale star-formation activity, it does not prove that 4C41.17 is 'primaeval'. Indeed, taken at face value, our results indicate that we are observing a massive starburst in 4C41.17 involving ~5–10% of its eventual stellar mass, as would be expected for a giant elliptical galaxy in the final stages of formation. None of the available data on 4C41.17 can yet distinguish whether star formation in 4C41.17 began at $z \approx 4$, or whether the bulk of its stellar content was formed at much higher redshifts. It remains entirely possible that the general population of elliptical galaxies was formed at $z > 10$, and that in high-redshift radio galaxies at $z \approx 3$–4 we are observing the final spectacular stages in the construction of luminous cD galaxies by mergers. □

Received 28 February; accepted 14 June 1994.

1. Sandage, A. *Astr. Astrophys.* **161,** 89–101 (1986).
2. Eales, S., Rawlings, S., Puxley, P., Rocca-Volmerange, B. & Kuntz, K. *Nature* **363,** 140–142 (1993).
3. Eales, S. A. & Rawlings, S. *Astrophys. J.* **411,** 67–88 (1993).
4. Dunlop, J. S. & Peacock, J. A. *Mon. Not. R. astr. Soc.* **263,** 936–966 (1993).
5. Tadhunter, C. N., Scarrott, S. M., Draper, P. & Rolph, C. *Mon. Not. R. astr. Soc.* **256,** 53P–58P (1992).
6. Boughn, S. P., Saulson, P. R. & Uson, J. M. *Astrophys. J.* **301,** 17–22 (1986).
7. Collins, C. A. & Joseph, R. D. *Mon. Not. R. astr. Soc.* **235,** 209–220 (1988).
8. De Propris, R., Pritchet, C. J., Hartwick, F. D. A. & Hickson, P. *Astr. J.* **105,** 1243–1250 (1993).
9. Thompson, D., Djorgovski, S. & Beckwith, S. V. W. *Astrophys. J.* (in the press).
10. Chambers, K. C., Miley, G. K. & van Breugel, W. *Astrophys. J.* **363,** 21–39 (1990).
11. Miley, G. K., Chambers, K. C., van Breugel, W. & Macchetto, F. *Astrophys. J.* **401,** L69–L73 (1992).
12. Carilli, C. L., Owen, F. & Harris, D. E. *Astr. J.* **107,** 480–493 (1994).
13. Hippelein, H. & Meisenheimer, K. *Nature* **362,** 224–226 (1993).
14. Graham, J. R. *et al. Astrophys. J.* **420,** L5–L8 (1994).
15. Soifer, B. T., Houck, J. R. & Neugebauer, G. *A. Rev. Astr. Astrophys.* **25,** 187–230 (1987).
16. Duncan, W. D., Robson, E. I., Ade, P. A. R., Griffen, M. J. & Sandell, G. *Mon. Not. R. astr. Soc.* **243,** 126–132 (1990).
17. Rowan-Robinson, M. *et al. Nature* **351,** 719–721 (1991).
18. Rowan-Robinson, M. *et al. Mon. Not. R. astr. Soc.* **261,** 513–521 (1993).
19. Hughes, D. H., Robson, E. I., Dunlop, J. S. & Gear, W. K. *Mon. Not. R. astr. Soc.* **263,** 607–618 (1993).
20. Chini, R., Kreysa, E. & Biermann, P. L. *Astr. Astrophys.* **219,** 87–97 (1989).
21. Draine, B. T. & Lee, H. M. *Astrophys. J.* **285,** 89–108 (1984).
22. Mathis, J. S. & Whiffen, G. *Astrophys. J.* **341,** 808–822 (1989).
23. Knapp, G. R. & Patten, B. M. *Astr. J.* **101,** 1609–1622 (1991).
24. Hines, D. C. & Wills, B. J. *Astrophys. J.* **415,** 82–92 (1993).
25. Heckman, T. M., Chambers, K. C. & Postman, M. *Astrophys. J.* **391,** 39–47 (1992).
26. Hughes, D. H., Gear, W. K. & Robson, E. I. *Mon. Not. R. astr. Soc.* **244,** 759–766 (1990).
27. Owen, F. N. & Laing, R. A. *Mon. Not. R. astr. Soc.* **238,** 357–378 (1989).
28. Solomon, P. M., Downes, D. & Radford, J. E. *Astrophys. J.* **398,** L29–L32 (1992).

ACKNOWLEDGEMENTS. We thank G. Miley and K. Meisenheimer for permission to reproduce their published images of 4C41.17, and the JCMT staff (Joint Astronomy Centre, Hilo) for their assistance with the observations. This research was supported by the award of an SERC post-doctoral research assistantship (D.H.H.), an SERC Advanced fellowship (S.R.), a NATO collaborative research grant (S.R. and S.E.), an operating grant from NSERC of Canada (S.E.) and a Connaught Award from the University of Toronto (S.E.).

Density and size of comet Shoemaker–Levy 9 deduced from a tidal breakup model

Johndale C. Solem

Theoretical Division, Los Alamos National Laboratory, Los Alamos, New Mexico 87545, USA

ALTHOUGH comets have been studied throughout most of recorded history, a detailed understanding of their internal properties is still lacking. Recent observations[1] of the split comet Shoemaker–Levy 9—actually a spectacular string of cometary fragments that resulted from the tidal disruption of a single parent body as it passed close to Jupiter[2–5]—have therefore stimulated much interest, as they provide an unprecedented opportunity to investigate the physical properties of comets more generally[6–8]. I report here simulations of the tidal breakup of the parent comet, which I assume to have been an assemblage of a large number of spherical components bound together only by gravity. Following the initial tidal disruption of the assemblage, the particles coalesce rapidly by mutual gravitation into a chain of larger fragments, the morphology of which depends critically on the density of the components. By comparing the size, number and distribution of the stimulated fragments with observations of Shoemaker–Levy 9, I determine an average comet density of about 0.5 g cm^{-3} and a parent comet diameter of about 1.8 km.

In contrast to the common view of a solid body[9], I model the comet as an agglomeration of individually competent components—'snowballs'—bound together only by mutual gravitational attraction. The depiction of comets as 'flying rubble piles' has enjoyed increasing support[6,10,11] and comets with multiple nuclei are not exceptional[12–14]. There are probably other cohesive forces between components, but I assume that these are small compared to gravitational binding.

In the simulations, the spherical components interact gravitationally except when they touch. The touching, or collision, of two components is handled as a non-adhesive dissipative scattering, that is, the velocities are suddenly changed in such a way that momentum is conserved, but some of the kinetic energy is converted to heat. The simulation is a detailed calculation of the gravitational interaction and collisions of the components—it is not a hydrodynamic calculation.

A further simplification, which greatly accelerates computation, is to assume that the radius r_0 and density ρ of each component is the same. Under this assumption, the equation of motion in the vicinity of the comet's centre of mass is well approximated by

$$\ddot{\mathbf{r}}_j = G\left[m_0 \sum_{i \neq j} \frac{\mathbf{r}_i - \mathbf{r}_j}{|\mathbf{r}_i - \mathbf{r}_j|^3} + \frac{2M(\mathbf{R} \cdot \mathbf{r}_j)\mathbf{R}}{R^5}\right] \quad (1)$$

where G is the universal gravitation constant, M is the jovian mass, m_0 is the component mass, $\mathbf{r}_i$ is the radius vector of the ith component from the comet's centre of mass, and $\mathbf{R}$ is the radius vector of the comet's centre of mass from the jovian

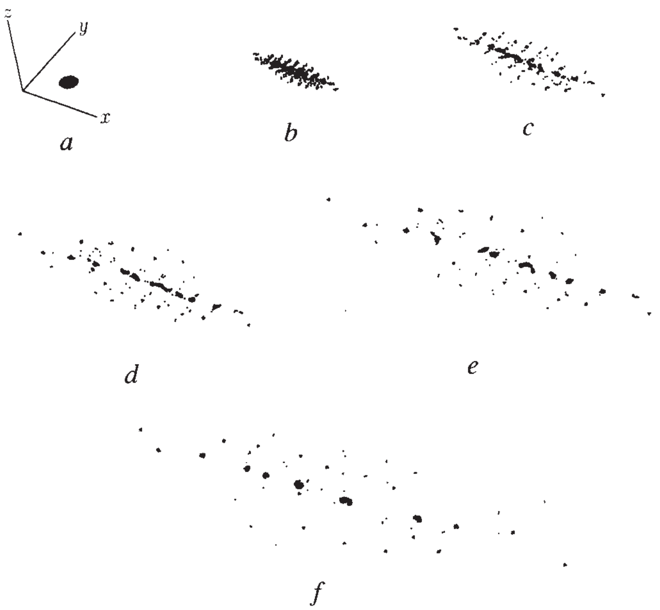

FIG. 1 *a–f*, Sequence of calculated configurations for the comet started at 2×10^4 s before perijove. *a*, Perijove; *b*, initial breakup of the comet 10^4 s after perijove; *c*, 2×10^4 s, coalescence is starting; *d*, 3×10^4 s, major fragments are forming; *e*, 4×10^4 sec; *f*, 5×10^4 s, most of the morphology is established.

centre. The first term of equation (1) is the net gravitational acceleration due to all the other components and binds the comet together. The second term is the acceleration due to the gradient in Jupiter's gravitational field and represents the tidal forces that pull the comet apart: components on the Jupiter side of the comet's centre of mass move toward the planet, whereas those on the opposite side move away.

As long as all the components remain separated by at least two radii, the motion is found by straightforward integration of equation (1). A 'collision' occurs whenever $|\mathbf{r}_i-\mathbf{r}_j|<2r_0$ and the emergent velocities are given by

$$\dot{\mathbf{r}}_i'=\dot{\mathbf{r}}_i-\frac{\delta(\dot{\mathbf{r}}_i-\dot{\mathbf{r}}_j)\cdot(\mathbf{r}_i-\mathbf{r}_j)}{8r_0^2}(\mathbf{r}_i-\mathbf{r}_j) \qquad (2)$$

A frictionless collision can only alter the normal component of

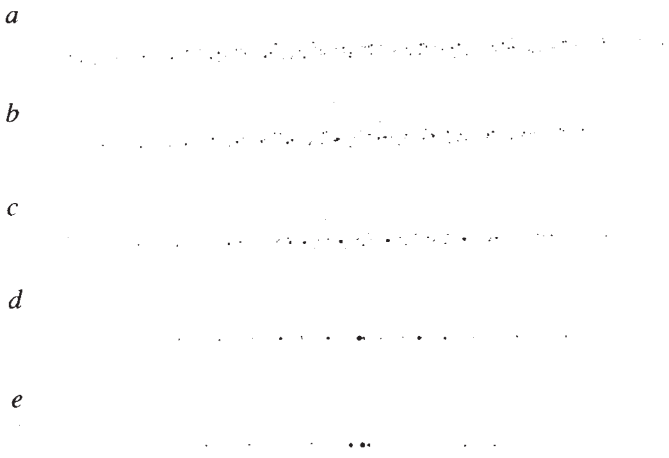

FIG. 2 *a–e*, Dependence of breakup on density of components. Configurations are shown at 10^5 s after perijove when size and relative position of the fragments are well established. Values of density (ρ) as follows (all g cm^{-3}): *a*, 0.45; *b*, 0.50; *c*, 0.55; *d*, 0.60; *e*, 0.65.

the relative velocity. If $\delta=2$, the normal component of the relative velocity simply reverses direction and the collision is perfectly elastic. If $\delta=1$, the normal component is reduced to zero in the collision. It is easy to see that the only allowed values are $1\leqslant\delta\leqslant2$.

We have little knowledge of how components of this sort might lose kinetic energy in collisions. For this calculation, the details are not very important. It can be shown that for completely random impact parameters, the selection of $\delta=1$ causes the average collision between components to lose half its relative kinetic energy to heat. This seems realistic. Because the gravitational orbital dynamics favour grazing collisions over random impact parameters, $\delta=1$ will result in slightly less than half energy loss on average.

The model embodied in equations (1) and (2) enjoys a remarkable scaling relationship: all distances scale with simple similarity. Locations are described by the dimensionless vector $\mathbf{r}_i/r_0$. If we increase the diameter of the comet by a factor of 2, the geometrical arrangement of all components at any time after disruption will be exactly the same, with the distance scale increased by a factor of 2. The energetics enjoy a similarly simple scaling relation. A factor of 2 increase in component radius increases all energies (kinetic energy, gravitational potential energy and heat generated in component collisions) by a factor of $2^5=32$. As a result of these scaling properties, we can cover comets of all sizes with a single calculation.

For the initial geometrical arrangement, I place one component at the centre of mass with 320 components packed around it in a face-centred cubic (f.c.c.) array, which results in a comet model that is close to a gravitational potential minimum. The time step for the dynamical calculation is adjusted so only binary collisions occur, although there may be many binary collisions among separate pairs within that time step. The lattice spacing for the spheres to just touch is $r_0\sqrt{2}$, but this contact packing would cause the binary-collision condition to be violated on the first time step. So I use an initial lattice spacing of $r_0(\sqrt{2}+0.0001)$—spheres are very close together, but not actually touching.

I approximate the encounter of Shoemaker–Levy 9 with Jupiter as a parabolic orbit with a closest approach (perijove) distance of 9.46×10^4 km (1.36 jovian radii) from the centre of the planet[15]. The orbit is obtained by integrating the newtonian equations of motion in the usual manner and describes the time-dependence of the location of the comet's centre of mass. Figure 1 shows the early stages of breakup as the comet passes Jupiter. Figure 1*a* depicts the comet at perijove and the directions of the cartesian coordinates. The orbital plane is parallel to the x–y plane and the x axis is parallel to the parabolic line of symmetry. The configurations are 10^4 s apart. The components have a density $\rho=0.55$ g cm^{-3} and are shown to scale. The sequence shows the initial pulverization of the comet by the tidal forces and subsequent coalescence into larger fragments by mutual gravitation.

Keeping the initial geometry the same, the fate of the comet is crucially dependent on its density. This sensitivity allows us to estimate the density from the comet's qualitative behaviour. For high densities, the binding term in equation (1) is always large compared to the tidal term, and the comet will not break up. For low densities, the comet will break into individual components, which simply disperse and never coalesce into larger objects. Figure 2 shows different breakup configurations resulting from identical initial geometry but different density. Each case is shown at 10^5 s after perijove, and with perspective approximately as it would be viewed from Earth. (Further coalescence and motion among the fragments result in only small morphological changes after 10^5 s.) At later times, the chain becomes long compared to the fragment size, so that it cannot be shown to scale. Because observational brightness is roughly proportional to cross-sectional area, I have chosen to make the comparisons at this relatively early time when the cross-sections

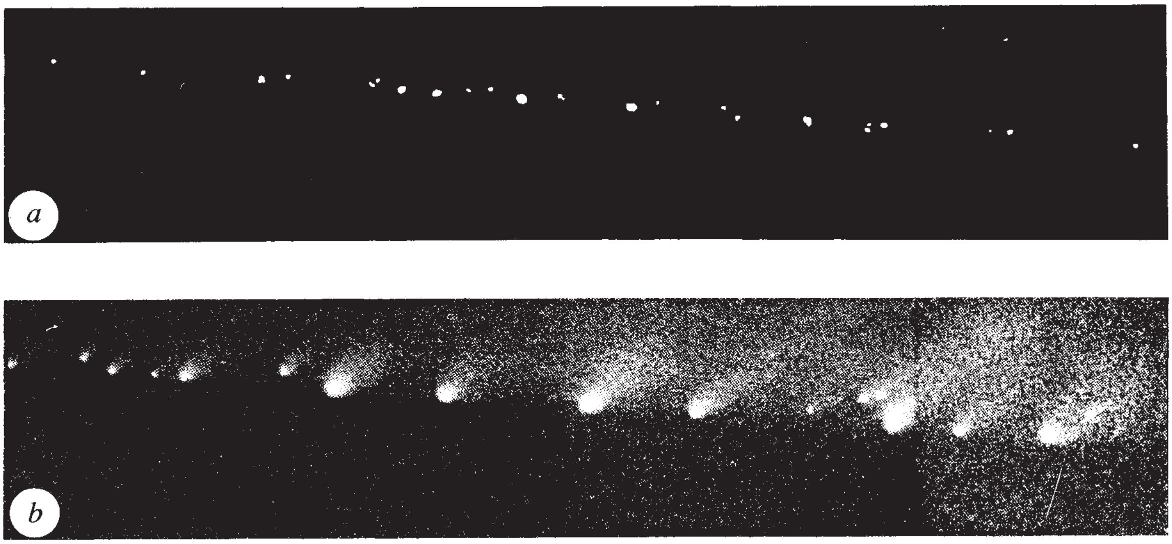

FIG. 3 *a*, *b*, Comparison between the brightness simulation from calculated breakup configuration shown as viewed from Earth at 10^6 s (*a*) and the observation of Shoemaker–Levy 9 by the Hubble telescope (*b*).

are still clearly visible. Ultimately, the length of the chain will increase with time t as $\sim t^{4/3}$ while its width will increase as $\sim t$. The chain will become thinner, but the size of the fragments and their relative spacing along the chain will remain the same.

Figure 2*c* is for $\rho = 0.55$ g cm^{-3} and corresponds most closely to the observed morphology of the comet chain. Figure 3*a* is a simulation of the relative brightness that would be observed from Earth for the $\rho = 0.55$ g cm^{-3} case at 10^6 s after perijove. The morphology is very similar to Fig. 2*c*, but some further coalescence has taken place. There is no coalescence between 5×10^5 s and 10^6 sec. Figure 3*a* shows a total of 23 fragments with 7 or 8 major fragments, in good agreement with the general description given of Shoemaker–Levy 9. Figure 3*b* is a reproduction of a recent Hubble observation[16]. The comparison is necessarily somewhat subjective.

Figure 2 suggests that the components have a density between 0.5 and 0.6 g cm^{-3}. The initial packing on an f.c.c. lattice makes the starting object a bumpy sphere. About 11% of the interior of the bumpy sphere is void, so the initial density of the comet is $\sim$0.5 g cm^{-3}.

For the calculations thus far presented, I have chosen $\delta = 1$. For $\delta = 2$, collisions between components are perfectly elastic, and once the components are dispersed by the tidal forces, they will never coalesce into larger fragments. A numerical simulation midway between the extremes, $\delta = 3/2$, gives a final configuration similar to the $\delta = 1$ case. The configuration can be brought into closer correspondence by a slight increase in density. The reason for the relative insensitivity is in part connected with the small fraction of energy that goes to heat.

The final configuration is also not very sensitive to the number of components in the initial configuration. Comets with larger numbers of components convert kinetic energy to heat more quickly, the rate going approximately as the one-third power of the number. A numerical simulation with 177 components produces a configuration qualitatively similar to the 321-component case, perhaps looking rather more like Fig. 2*b*. A broader study of the variation shows that a substantial increase in the number of components can be compensated by a slight decrease in density.

Initial rotation of the comet can have a more serious effect on the morphology. The angular velocity at which the gravitationally bound comet will be torn apart by centrifugal force is $\omega_c \approx \sqrt{Gm/r^3}$, where m is the comet's mass and r is its radius. So ω_c sets an upper limit on the rotational speed. From numerical simulations, I find that an initial angular velocity of $\omega_c/3$ will introduce a density-estimate uncertainty of ± 0.05 g cm^{-3}, which is as much accuracy as I could claim from the qualitative comparison anyway. Thus if the initial angular velocity of Shoemaker–Levy 9 is $< \omega_c/3$, the quantitative results given in this Letter should stand. We have very little information on the rotation of comets, but sparse information on asteroids shows few rotating near their centrifugal limit.

Because of the scaling of equations (1) and (2), I can very roughly estimate the initial size of of the comet from the length of the string of fragments. For a parabolic orbit at late times, it can be shown that $|\mathbf{r}_k - \mathbf{r}_l| \propto t^{4/3}$, where k and l are the furthest separated components. At 10^6 s after perijove, the numerical calculation gives $|\mathbf{r}_k - \mathbf{r}_l| = 2.4 \times 10^4 r_0$ and the 321-component f.c.c. bumpy sphere has a greatest diameter of $16.42 r_0$. On 1993 March 26.3 (2.26×10^7 s after perijove when the orbit was still reasonably parabolic) the string length was observed to be 1.64×10^5 km, which implies $r_0 = 1.1 \times 10^{-1}$ km and an initial diameter of 1.8 km, somewhat smaller than the diameter obtained by Scotti and Melosh[6] using a perijove distance of 1.57 jovian radii.

Note added in proof: Using a related model that included gravity but no collisions, Asphaug and Benz (*Nature* **370,** 120–124, 1994) obtained similar density constraints for the parent comet. □

Received 5 May; accepted 14 July 1994.

1. Shoemaker, C. S., Shoemaker, E. M. & Levy, D. H. *IAU Circ. No.* 5725 (1993).
2. Nakano, S. *IAU Circ. No.* 5800 (1993).
3. Marsden, B. G. *IAU Circ. No.* 5800 (1993).
4. Yeomans, D. K. & Chodos, P. *Minor Planet Circ. No.* 22197 (1993).
5. Yeomans, D. K. & Chodos, P. *IAU Circ. No.* 5909 (1993).
6. Scotti, J. V. & Melosh, H. J. *Nature* **365,** 733–735 (1993).
7. Boss, A. P. *Icarus* (submitted).
8. Sekanina, Z., Chodos, P. W. & Yeomans, D. K. *Astr. J.* (submitted).
9. Dobrovolskis, A. R. *Icarus* **88,** 24–38 (1990).
10. Weissman, P. *Nature* **320,** 242–244 (1986).
11. Weidenschilling, S. J. *Nature* **368,** 721–723 (1994).
12. Sekanina, D. & Yeomans, D. K. *Astr. J.* **90,** 2335–2352 (1985).
13. Sekanina, D. *Science* **262,** 382–387 (1993).
14. Whipple, F. L. in *The Mystery of Comets* Ch. 17 (Smithsonian Instn, Washington, 1985).
15. Chodas, P. W. & Yeomans, D. K. Jet Propulsion Lab. e-mail bulletin, INTERNET (jplinfo.jpl.nasa.gov), April 22, 1994.
16. Friend, T. *USA Today* 8 March, page 5D (1994).

ACKNOWLEDGEMENTS. The author acknowledges helpful conversations with T. J. Ahrens and B. G. Marsden.